Tribological Behavior of 316L Stainless Steel Reinforced with CuCoBe + Diamond Composites by Laser Sintering and Hot Pressing: A Comparative Statistical Study

Ângela Cunha[1], Ana Marques[1], Francisca Monteiro[1(✉)], José Silva[1], Mariana Silva[1], Bruno Trindade[2], Rita Ferreira[1], Paulo Flores[1], Óscar Carvalho[1], Filipe Silva[1], and Ana Cristina Braga[3]

[1] CMEMS – Center for Microelectromechanical Systems, University of Minho, Azurém 4800-058, Guimarães, Portugal
{id8694, id8696, id8700, id8693, id8692}@alunos.uminho.pt, rita.mac.ferreira@gmail.com, {pflores, oscar.carvalho, fsamuel}@dem.uminho.pt

[2] CEMMPRE – Center for Mechanical Engineering, Materials and Processes, University of Coimbra, Rua Luís Reis Santos, 3030-788 Coimbra, Portugal
bruno.trindade@dem.uc.pt

[3] ALGORITMI Research Centre, University of Minho, Guimarães, Portugal
acb@dps.uminho.pt

Abstract. The aim of this work was to perform a statistical analysis in order to assess how the tribological properties of a laser textured 316L stainless steel reinforced with CuCoBe - diamond composites are affected by diamond particles size, type of technology (laser sintering and hot pressing) and time of tribological test. The analysis started with the description of all response variables. Then, by using IBM® SPSS software, the Friedman's test was used to compare how the coefficient of friction varied among samples in five-time points. From this test, results showed that there was no statistically significant difference in the coefficient of friction mean values over the selected time points. Then, the two-samples Kolmogorov-Smirnov (K-S) test was used to test the effect of the diamond particles size and the type of technology on the mean of the coefficient of friction over time. The results showed that, for both sintering techniques, the size of the diamond particles significantly affected the values of the coefficient of friction, whereas no statistical differences were found between the tested sintering techniques. Also, the two-way ANOVA test was used to evaluate how these factors influence the specific wear rate, which conducted to the same conclusions drawn for the previous test. The main conclusion was that the coefficient of friction and the specific wear rate were statistically affected by the diamond particles size, but not by the sintering techniques used in this work.

Keywords: Statistical analysis · Tribological behavior · Selective Laser Sintering · Hot pressing · Multi-material surface

© Springer Nature Switzerland AG 2020
O. Gervasi et al. (Eds.): ICCSA 2020, LNCS 12251, pp. 231–246, 2020.
https://doi.org/10.1007/978-3-030-58808-3_18

1 Introduction

Austenitic stainless steels are characterized by high applicability in the mechanical, chemical and process industries [1] due to their high resistance to corrosion, high strength and machinability [2–4]. In the automotive industry, the 316L stainless steel is a candidate to substitute the ductile or cast iron in the fabrication of piston rings [5], since it presents similar chemical composition and has an inherent strength that leads to a less chance of ring breakage, with consequently longer service life. The surface of a piston ring must be multifunctional. The reduction of the friction, the retention of oil during operation, the retention of particles from wear and the increase in the thermal conductivity are target properties in the development of automotive piston rings [6, 7]. The 316L stainless steel has low wear resistance, which can be improved by the addition of hard ceramic particles on the surface [8–10]. Different metallic and ceramic material have been used as reinforcements of metallic matrices such as tungsten [11, 12], titanium [12, 13], silicon and niobium carbides [8, 14] and diamond [15, 16] to produce metal matrix composites (MMCs). These composites materials present exceptional combination of properties and performance [11, 17] with improved mechanical and tribological properties when compared with the matrix [13, 18]. The processing temperature of diamond-reinforced MMCs is an important issue because graphitization of diamond into graphite occurs at 900 °C [15, 16, 19]. So, low-temperature processing techniques are required for the production of these materials. In previous work, a laser-textured 316L steel was reinforced with CuCoBe-diamond composites through selective laser sintering (SLS) and hot pressing (HP) [20, 21]. The results showed that the tribological properties of the 316L steel were improved by the reinforcement composite. Selective Laser Sintering (SLS) is an additive manufacturing (AM) process that presents an extraordinary versatility to geometry and materials design, as it is considered a near-net-shape technology [22, 23]. It is also characterized by being a fast technique, which is a potential advantage in mass production. On the other hand, Hot Pressing technique, characterized by the simultaneous application of temperature and pressure, allows obtaining well-consolidated components with high mechanical performance due to the low porosity that it presents [24, 25]. When using pressure and temperature simultaneously, it is possible to compensate temperature with pressure, using lower temperatures. In this case, it is important due to the graphitization of the diamond temperature.

This work aims to study, through statistical analysis, the influence of the two consolidation technologies (SLS and HP) on the tribological behavior of laser-textured 316L samples reinforced with CuCoBe-diamond composites. The size effect of the diamond particles on the tribological properties will also evaluated and discussed.

2 Methodology Procedure

2.1 Materials and Processing Details

Samples of SS316L with 14 mm diameter were textured through an Nd:YAG laser (Sisma Laser) with a wavelength of 1064 nm, laser power of 6 W, scan speed of

128 mm/s, number of passes of 16 and fill spacing of 5 μm. The texture produced (see Fig. 1) was analyzed by scanning electron microscopy (SEM) (Nano-SEM - FEI Nova 200 equipment) and 3D profilometry (InfiniteFocus from Brucker alicona).

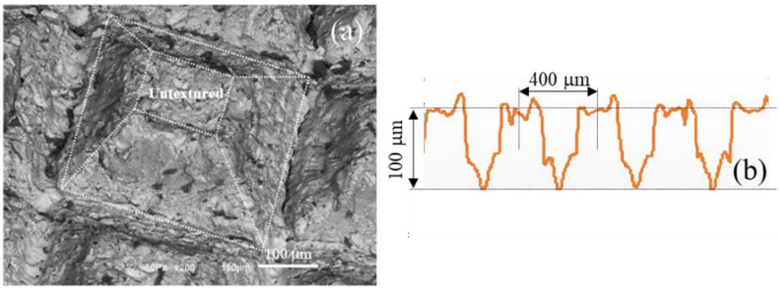

Fig. 1. Texture produced: (a) SEM image of the textured and (b) heights of the profile produced.

The CuCoBe (1.5 wt% cobalt, 0.5 wt% beryllium and the remainder is copper) + 5.8 wt% diamond composites were produced by mechanical alloying (MA) from elemental powders. Two different grades of diamond particles (0.1–0.5 μm and 40–60 μm) were used. The powder size of the CuCoBe alloy was 40–80 μm. Five different samples were produced by laser sintering and hot pressing in this work (Table 1).

Table 1. Samples produced and analyzed in this work.

Sample reference	Description
316L + C_0.1–0.5 (SLS)	Textured 316L stainless steel reinforced with mechanical alloyed CuCoBe + diamond particles (0.1–0.5 μm) produced by SLS
316L + C_40–60 (SLS)	Textured 316L stainless steel reinforced with mechanical alloyed CuCoBe + diamond particles (40–60 μm) produced by SLS
316L + C_0.1–0.5 (HP)	Textured 316L stainless steel reinforced with mechanical alloyed CuCoBe + diamond particles (0.1–0.5 μm) produced by HP
316L + C_40–60 (HP)	Textured 316L stainless steel reinforced with mechanical alloyed CuCoBe + diamond particles (40–0 μm) produced by HP

Figure 2 shows a schematic representation of the two processes used for the reinforcement of the textured 316L stainless steel, SLS and HP.

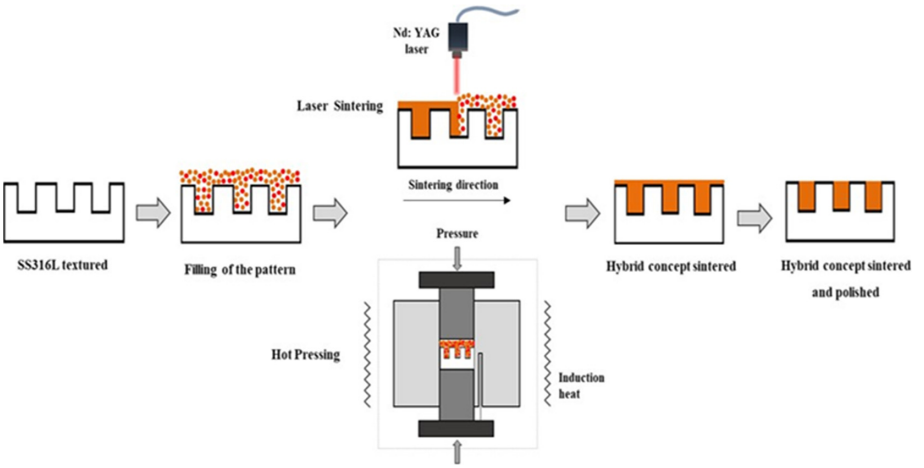

Fig. 2. Schematic representation of the two processes used for the reinforcement of the textured 316L.

For SLS, samples were sintered through the same laser, power and scan speed used for texturing but using just 1 pass and a fill spacing of 20 μm. Under these conditions one line affects a distance of 27 μm, so with the fill spacing used, overlapping of the lines was ensured and consequently sintering of the entire surface was performed. Regarding HP, the process was conducted using a vacuum pressure-assisted sintering system (under a vacuum of 1×10^{-4} Pa) with a high-frequency induction furnace. Samples were heated up to 900 °C, with a heating rate of 100 °C/min, and an applied pressure of 70 MPa, for 30 min. The samples were then cooled down to the room temperature.

After sintering, a polishing operation was necessary to expose the 316L steel surface. The samples were polished with SiC abrasive papers down to a 4000 mesh and ultrasonically cleaned with isopropyl alcohol before tribological tests.

2.2 Tribological Tests

A reciprocating pin-on-plate tribometer (see Fig. 3) was used (Plint TE67-HT) for the tests, which replicates the piston ring-cylinder liner contact. The pin (counter body) consisted of a malleable cast iron cylindrical body with a diameter of 2.25 mm (geometry similar to the engine cylinder body).

The test conditions were defined based on the engine's operating conditions (similar to the in-service conditions) and in accordance with the restrictions of the test equipment. The wear sliding tests were performed dry at 25 N loading (nominal), with a frequency of 1.5 Hz and 7 mm of total stroke length for 4 h. The contact area

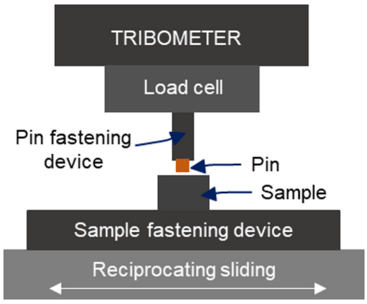

Fig. 3. Schematic representation of the tribological tests.

between two components (pin and sample) was 3.98 mm^2, resulting in contact pressure of 6.29 N/mm^2. Three samples were produced for each processing condition. For each processing condition, three tribological tests were performed and the mean and standard deviation were calculated.

From the tests it was possible to obtain the COF directly and, in addition, the mass loss of the sample was determined (difference between the initial and the final mass). The mass loss and the density of the materials allowed to determine the wear volume (w) in mm^3. So, the specific wear rate (k) of the surfaces was calculated according to the Eq. 1.

$$k = \frac{w}{F_n \cdot s} \tag{1}$$

where F_n represents the normal force in N (25 N) and s is the sliding distance in m (≅284 m).

It should be noted that while the COF variable is measured over time, the variable specific wear rate is a unique value, measured at the end of each test.

2.3 Statistical Analysis

The general procedure followed in this statistical study is schematically presented in Fig. 4. A significance level of 5% was considered for all the statistical analysis.

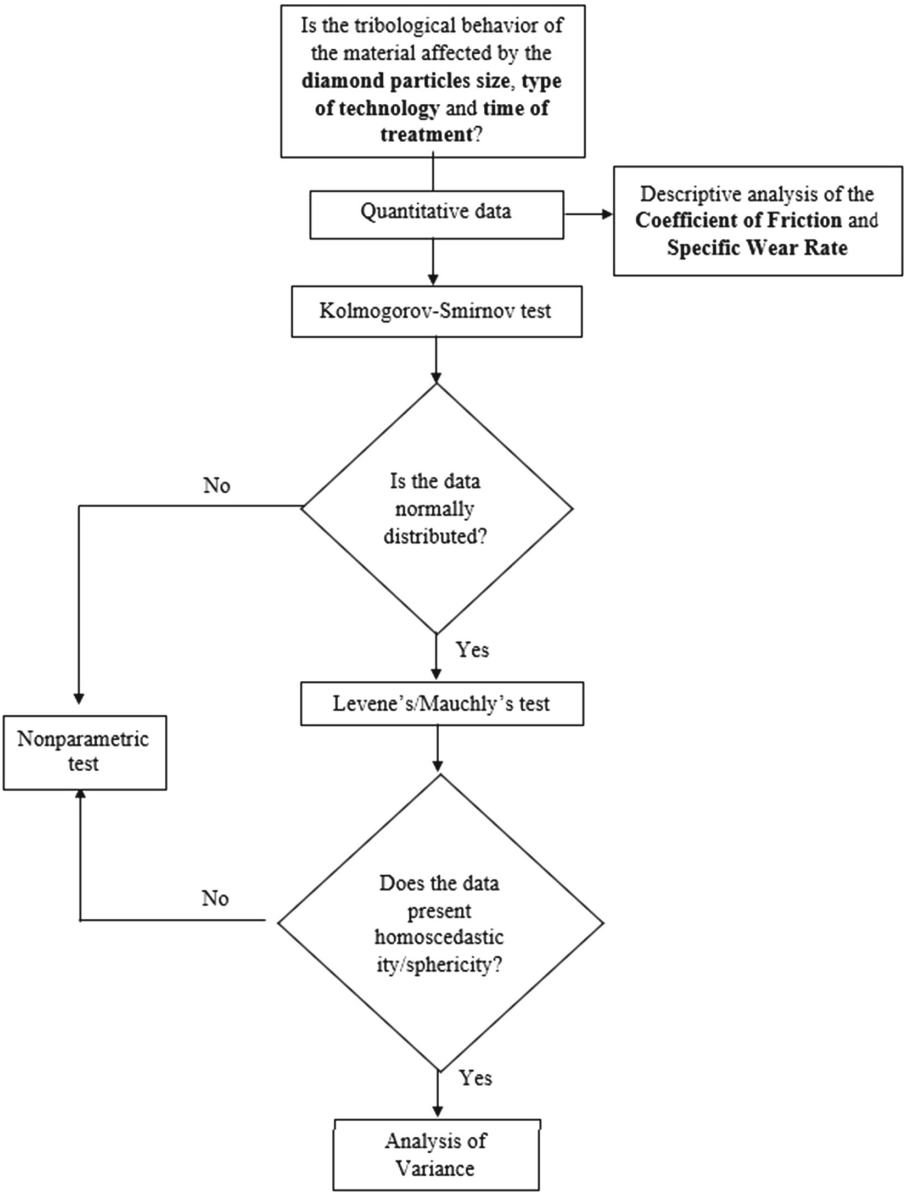

Fig. 4. Flowchart of the methodology adopted for the statistical analysis.

3 Statistical Analysis and Discussion of Results

3.1 Descriptive Analysis of COF

In this section, a statistical study of the dependent variable, coefficient of friction (COF), in each sample [316L + C_0.1–0.5 (SLS), 316L + C_40–60 (SLS), 316L + C_0.1–0.5 (HP) and 316L + C_40–60 (HP)] is presented considering each trial. It was carried out in IBM® SPSS software. Three trials per sample were executed. The obtained results are presented in Table 2.

Table 2. Statistics for each sample considering each trial for COF.

Material		Statistics			
		Mean	Median	Std. Deviation	Skewness
316L + C_0.1–0.5 (SLS)	Trial 1	0.4690	0.4637	0.2112	0.2600
	Trial 2	0.4327	0.4324	0.0087	0.1040
	Trial 3	0.4484	0.4574	0.0242	−0.7920
316L + C_40–60 (SLS)	Trial 1	0.1195	0.1192	0.0029	0.3620
	Trial 2	0.1309	0.1305	0.0033	0.3000
	Trial 3	0.1320	0.1326	0.0035	0.2120
316L + C_0.1–0.5 (HP)	Trial 1	0.5837	0.5939	0.0460	−0.3820
	Trial 2	0.5446	0.5313	0.0286	0.2970
	Trial 3	0.4926	0.4930	0.0115	−0.3280
316L + C_40–60 (HP)	Trial 1	0.1383	0.1375	0.0039	0.6160
	Trial 2	0.1572	0.1567	0.0034	0.5350
	Trial 3	0.1158	0.1145	0.0064	0.8220

The descriptive statistics of each sample considering the three trials performed is discussed. An example is given for Trial 2 of 316L + C_0.1–0.5 (SLS). The same analysis is applicable to Trials 1 and 3, as well as to other samples. Trial 2 presents a mean and median of 0.4327 and 0.4324, respectively. This leads to the conclusion that, for Trial 2, the mean COF value is 0.4327 and half the COF values are less than or equal to 0.4324.

COF's skewness for Trial 2 (0.1040) mirrors an approximately symmetric distribution.

Comparing all histograms from the samples, it is possible to conclude that Trial 1 is the worst regarding to its distribution. This might have due to some aspects of the experiments performed. The same counter body was utilized for all trials. In Trial 3, the counter body has a smoother surface with fewer asperities than in Trials 1 and 2, and fewer rough edges are encountered. Therefore, the contact between the two materials (counter body and sample) becomes more uniform. Due to this fact, the relative movement is more easily maintained when compared to Trials 1 and 2. In Trial 1, the surfaces of the counter body and sample are more irregular at a microscopic level (larger number and size of asperities) and therefore there is higher resistance. This leads

to higher difficulty in sliding and consequently, a distribution for COF that is not close to normality. Over time and trials, less rough edges exist, and the track adapts to the counter body geometry, leading to better distribution for COF in Trial 3.

3.2 Descriptive Analysis of Specific Wear Rate

In this section a statistical study of the dependent variable, specific wear rate (k), for each sample [316L + C_0.1–0.5 (SLS), 316L + C_40–60 (SLS), 316L + C_0.1–0.5 (HP) and 316L + C_40–60 (HP)] is presented. The analysis was carried out in IBM® SPSS software, and the obtained results are presented in Table 3.

Table 3. Statistics for each sample considering each trial for k.

Sample	Statistics			
	Mean	Median	Std. Deviation	Skewness
316L + C_0.1–0.5 (LS)	0.00002733	0.00002410	0.00000862	1.451
316L + C_40–60 (LS)	0.00000236	0.00000265	0.00000223	−0.583
316L + C_0.1–0.5 (HP)	0.00001180	0.00001200	0.00000111	−0.782
316L + C_40–60 (HP)	0.00000058	0.00000109	0.00000148	−1.356

From the results obtained, it is possible to conclude that the 316L + C_0.1–0.5 (SLS) sample has the highest mean value of the specific wear rate. Contrarily, the 316L + C_40–60 (HP) sample is the one presenting the lowest specific wear rate. Considering the effect of the particle size, these results show that the samples with higher particles sizes are more resistant to wear than samples with lower particles sizes. Regarding the median value, the 316L + C_40–60 (HP) sample experienced the lowest value for this statistic, meaning that 50% of this sample is subjected to less wear than 50% of the other samples during the performed trials. These results corroborate the above-mentioned conclusion on the mean value for k.

Regarding the skewness statistic for the analysis of k, only one sample [316L + C_0.1–0.5 (SLS)] has a right skewed distribution, with the remaining samples comprising left skewness. Taking the above assumptions in consideration, it can be said that the distribution of 316L + C_0.1–0.5 (SLS) is highly skewed to the right, that is, its right tail is longer than the left tail, and the k distribution is more concentrated on the left side. This is corroborated by the fact that the mean k value for this sample is higher than the median value, which in turn is higher than the mode ($0.00002733 > 0.00002410 > 0.00002080$). Amongst samples comprising a left skewed distribution and considering the previously referred assumptions, the 316L + C_40–60 (SLS) and 316L + C_0.1–0.5 (HP) ones present a moderately left skewed distribution, and the 316L + C_40–60 (HP) one has a highly left skewed distribution.

3.3 Differences of the Measurement of COF Through Time

Problem. In order to assess if there is a statistically significant difference of COF values of the samples with respect to time, five different time points were selected among the time range. Table 4 presents the five different time points, and the COF values for the four different material conditions, each with three samples, resulting in a total of twelve different conditions.

Table 4. COF values of the four different samples at the five time points.

Sample	Time (s)				
	3600	6300	9000	11700	14397
316L + C_0.1–0.5 (SLS)	0.4473	0.4423	0.4621	0.4837	0.5058
	0.4389	0.4294	0.4389	0.4384	0.4351
	0.4109	0.4252	0.4463	0.4755	0.4654
316L + C_40–60 (SLS)	0.1255	0.1215	0.1192	0.1165	0.1162
	0.1383	0.1383	0.1300	0.1297	0.1250
	0.1389	0.1330	0.1330	0.1280	0.1270
316L + C_0.1–0.5 (HP)	0.4980	0.5643	0.5919	0.6355	0.6406
	0.5144	0.5142	0.5262	0.5825	0.5928
	0.4888	0.4806	0.4905	0.5034	0.4847
316L + C_40–60 (HP)	0.1484	0.1408	0.1344	0.1383	0.1379
	0.1629	0.1607	0.1564	0.1579	0.1556
	0.1288	0.1187	0.1113	0.1087	0.1187

Resolution. In order to study the influence of time in the response variable (COF of the four different samples), the first method attempted was the repeated measures ANOVA. This method eliminates sources of variability between subjects on the experiment error [26]. Therefore, the null hypothesis (H_0) for this test, is given as follows:

H_0: The COF mean values are equal at different time points.

The method implies that the response variable has to be normally distributed within each time points, and sphericity must be guaranteed. Considering the Mauchly's test, $\chi 2$ (4) = 2.760, p-value = 8.66e−09 (p-value < 0.05), the assumption of sphericity is rejected for a significance level of 5%. Corrections could be performed to overcome the violation of sphericity.

Regarding the violation of the normally distributed data assumption (p-value < 0.05), the analysis of variance between time points was again conducted, although with the Friedman test - a non-parametric test [27]. The null-hypothesis and the alternative hypothesis, for this test, are the same as the ones formulated for the repeated measurements ANOVA test. The Friedmann's test is described by Eq. 2 [27].

$$\chi^2 = \frac{12n}{p(p+1)} \sum_{j=1}^{p} \left\{ \bar{r}_j - \frac{1}{2}(p+1) \right\}^2 \quad (2)$$

where $\bar{r}_j$ is the mean rank of the jth time point, p is the number of ranks (time points) and n the number of rows (total number of samples). If χ^2 is too high, then the mean ranks differ significantly [27].

The statistics for this test, $\chi^2(4) = 3.800$, p-value = 0.434 (p-value > 0.05), do not reject the null hypothesis of the COF mean values being equal through all the time points. This outcome enables to consider the mean values of COF, through all the time points, for further analysis.

3.4 Effects of Factors on the COF

Problem. The aim of this statistical analysis was to understand how the diamond particles size and the type of technology used in each sample affect the COF. Having this in mind, both levels of each factor were considered and the mean COF over time from the three trials (Table 5) was tested for each combination of factors.

Table 5. Means of COF for each of the three trials over time, for the four samples.

		Diamond particles size (factor A)	
		0.1–0.5 μm	40–60 μm
Type of Technology (factor B)	HP	0.46897; 0.43269; 0.44838	0.11947; 0.13091; 0.13196
	SLS	0.58369; 0.54460; 0.49262	0.13831; 0.15715; 0.11585

Resolution. This two-factor experiment has 12 observations (2 diamond particles sizes x 2 technologies of sintering x 3 trials). In order to test the significance of the effect of each factor, the first attempt was to apply the Analysis of Variance (ANOVA) method with a two-factor factorial design. Firstly, for the application of this method, its assumptions must be satisfied, namely the response variable (mean of COF over time) has to be normally distributed; homoscedasticity has to be verified; as well as randomness of the data [26]. To check the normality of the data, the Kolmogorov-Smirnov (K-S) test was used.

Accordingly, the K-S test points to the same conclusion, as $D(12) = 0.290$, $p\text{-value} = 0.006$ (p-value < 0.05), therefore rejecting the null hypothesis.

Given that one of the ANOVA assumptions is not fulfilled, it was necessary to resort to another statistical method, in this case, a nonparametric method. Since the response variable presents different variabilities for each combination of factors' levels, a test to compare the distribution of two independent samples was chosen - the two-sample K-S test. The respective statistic, $D_{m,n}$, is calculated as presented in Eq. 3 [28].

$$D_{m,n} = \sup_{|x|<\infty} \left|\hat{F}_{1m}(x) - \hat{F}_{2n}(x)\right| \quad (3)$$

where m and n are the samples sizes, x is the response variable; and $\hat{F}_{1m}(x)$ and $\hat{F}_{2n}(x)$ are the empirical distribution functions obtained from each sample.

Regarding diamond particles size, by applying this method, it was possible to conclude that the distribution of COF across the 0.1–0.5 μm and 40–60 μm diamond particles is not the same, since the software returned the results of *D(12) = 1.732*, *p-value* (2-sided test) = *0.005*. In contrast, the results that concern to the type of technology point to a similar distribution of COF across HP and SLS technologies, as *D(12) = 0.866*, *p-value* (2-sided test) = *0.441*.

Therefore, on the basis of the two-samples K-S test, it is possible to conclude that the diamond particles sizes used in the sintering process produced a statistically significant impact in COF (p-value < 0.05), since the two particles sizes induced a statistically different effect on the response variable for both technologies of sintering. Contrarily, the type of technology did not affect COF in a statistically significant way (p-value > 0.05).

3.5 Effects of Factors on the Specific Wear Rate (*k*)

Problem. The main goal of this statistical analysis was to study the effects of the diamond particles size and type of technology on the specific wear rate of the sample. Table 6 presents the two levels of each factor considering the combination of factors.

Table 6. *k* values for each of the three trials, for the four samples.

		Diamond particles size (factor A)	
		0.1–0.5 μm	40–60 μm
Type of Technology	HP	3.71e−05; 2.41e−05; 2.08e−05	4.42e−06;0.00e+00; 2.65e−06
	SLS	1.20e−05; 1.28e−05; 1.06e−05	−1.09e−06; 01.75e−06; 1.09e−06

The negative value of *k* observed for the SLS samples with particle size of 40–60 μm means that the counter body had transferred mass to sample. The null value of *k* observed for the same particle size using HP for the same particle size means that there is an equilibrium between the mass transferred from counter body to sample and from to sample to counter body.

Resolution. Again, the ANOVA method was performed in order to test the significance of the effect of particle size and technology type. However, the same assumptions previously described need to be verified. The normality of the data was checked by performing the K-S test.

The null hypothesis is not rejected [*D(12) = 0.198* and *p-value = 0.200* (p-value > 0.05)] and therefore the *k* data follow a normal distribution. The homoscedasticity was also checked by performing the Levene's test, from which it was possible to confirm the homogeneity of variance, once the obtained p-values were of 0.15 and 0.20 for

different technologies [*D(12) = 8.590*] and diamond particles sizes [*D(12) = 7.573*], respectively.

Considering a full factorial model, the analysis of interactions and factors was performed. The effect of each factor indicates a variation in the response variable due to the change in the levels of particle size or technology type. An interaction between the two factors is verified when the effect on one factor depends on the condition of the other factors.

The interaction between particle size and type of technology (H_{03}) was observed since for *F(1,8) = 6.872* the p-value obtained was 0.031 (p-value < 0.05), and so the null hypothesis is rejected. Therefore, it can be concluded that the interaction between particle size and technology type affects the *k*. Since an interaction was observed, the analysis of main effects does not explain correctly the effect of factors on the response variable.

The high value of R squared ($R^2 = 0.891$) obtained on the ANOVA test means that the relation between the response variable, the levels of factors and the interaction are well explained by the model. The same conclusion can be taken by observing the corrected value (p-value $\sim$ 0.00 < 0.05) on ANOVA table once there is a significative statistical relation. Additionally, the low value of the error (2.067e-11) mirrors the variability of the residuals, which corresponds to the random errors that models cannot explain. Therefore, this allows to conclude that, in fact, there is an interaction.

Figure 5 presents the interaction plot that displays the fitted values of the *k* variable on the y-axis and the particle size values on the x-axis. The two lines represent the technology types.

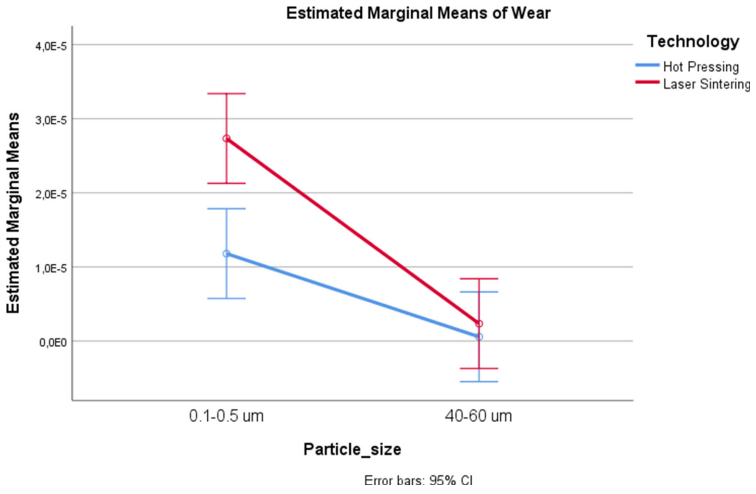

Fig. 5. Interaction effect between particle sizes for two technologies considered.

The different slopes propose that there is an interaction effect, which is confirmed by the p-value for the particle size/technology type. Also, from the distances between

the segment edges, it is possible to see that, for smaller particles, there are significative differences between technologies, while for bigger particles this is not verified, suggesting that the behavior of the factor levels changes with type of technology used.

Additionally, the normality of the residuals was checked by performing the K-S test.

The null hypothesis is not rejected [$D(12) = 0.215$ and $p\text{-}value = 0.102$ (p-value > 0.05)] and therefore the k data follow a normal distribution.

The homoscedasticity of the residuals was checked by performing the Levene's test. The plot of residuals against estimated values of k is shown in Fig. 6. The results of Levene's test confirm the homoscedasticity. A p-value of 0.102 for $D(12) = 0.215$ was obtained and therefore the null hypothesis is not rejected. The homogeneity of variance can be also confirmed by a satisfactory pattern in the referred plot. However, the Fig. 6 reveals a funnel pattern for residuals, which means that there are anomalies in the data.

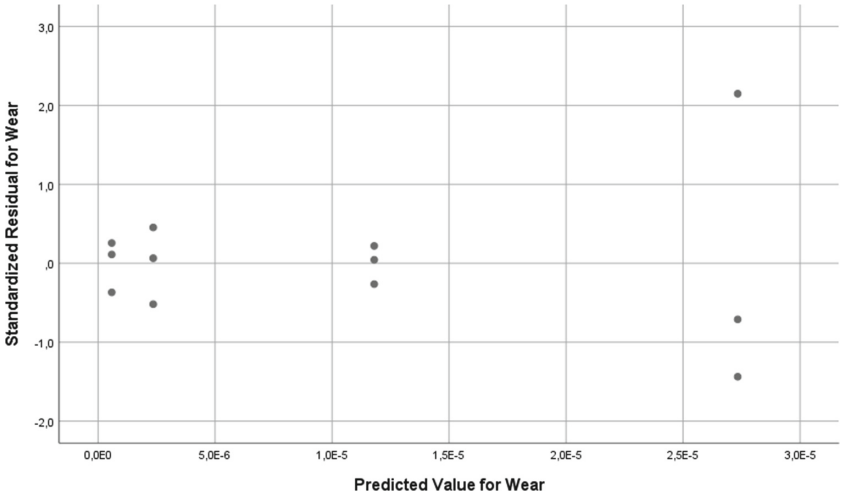

Fig. 6. Plot of residuals against estimated values of k.

In order to understand the anomalies verified in the previous graph, a boxplot of two diamond particles sizes and two type of technologies (Fig. 7) was executed. The graph allowed to conclude that the non-satisfactory pattern might be due to the large dispersion observed for particle size of 0.1–0.5 μm and SLS technology, when compared to the other conditions. No outliers exist in the data.

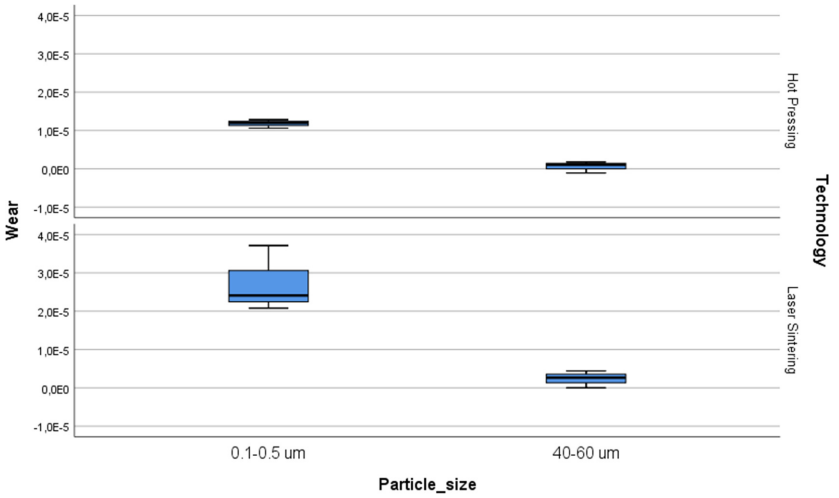

Fig. 7. Boxplot of two diamond particles sizes and two type of technologies.

As mentioned during ANOVA table analysis, the high value of R^2 revealed a well explained model. The corrected model with p-value lower than significance level proves a significative statistical relation and the Levene's a variance homogeneity. So, considering these points and the variability on boxplots, the anomalies found on residuals should not be considered relevant.

4 Conclusions

The modification of the tribological properties of laser textured 316L stainless steel reinforced with a CuCoBe-diamond composites was investigated in this work. After performing the descriptive analysis of the data, five time points were analyzed using the Friedman's test in order to assess the effect of time in the COF. Significant differences were found between the tested time points, suggesting that the reinforcement with diamond particles and the sintering technology affect the COF over time. Then, the ANOVA method with a two-factor factorial design was applied to study how two factor – the diamond particles size and the type of technology – affected the COF. It was found that the diamond particles size significantly impacts the referred parameter, whereas the type of treatment does not produce a significant effect on COF value. Finally, regarding the effects of the factors on the k, a high value of R^2 was obtained in the ANOVA test. This indicates an adjusted model to describe the relation between the response variable, the factors levels and their interaction. Based on the evidences provided in this paper, further statistical assessments must be performed in the topic to investigate the impact of more diamond particle sizes and types of technology on the COF and k, which would allow a more conscious and assertive implementation of such methodologies in specific environments.

Acknowledgements. This work was supported by FCT national funds, under the national support to R&D units grant, through the reference projects UIDB/04436/2020; UIDP/04436/2020; UIDB/00319/2020; and PTDC/CTM-COM/30416/2017.

References

1. Xavior, M.A., Adithan, M.: Determining the influence of cutting fluids on tool wear and surface roughness during turning of AISI 304 austenitic stainless steel. J. Mater. Process. Technol. **209**(2), 900–909 (2009)
2. Mahathanabodee, S., Palathai, T., Raadnui, S., Tongsri, R., Sombatsompop, N.: Dry sliding wear behavior of SS316L composites containing h-BN and MoS 2 solid lubricants. Wear **316**(1–2), 37–48 (2014)
3. Baddoo, N.R.: Stainless steel in construction: A review of research, applications, challenges and opportunities. J. Constr. Steel Res. **64**(11), 1199–1206 (2008)
4. Yan, F.K., Liu, G.Z., Tao, N.R., Lu, K.: Strength and ductility of 316L austenitic stainless steel strengthened by nano-scale twin bundles. Acta Mater. **60**(3), 1059–1071 (2012)
5. Yamagata, H.: The Piston Ring. The Science and Technology of Materials in Automotive Engines, pp. 87–109. Woodhead Publishing (2005)
6. Zabala, B., et al.: Friction and wear of a piston ring/cylinder liner at the top dead centre: Experimental study and modelling. Tribol. Int. **106**, 23–33 (2017)
7. Carvalho, O., Buciumeanu, M., Madeira, S., Soares, D., Silva, F.S., Miranda, G.: Optimization of AlSi – CNTs functionally graded material composites for engine piston rings. Mater. Des. **80**, 163–173 (2015)
8. Kan, W., et al.: A study on novel AISI 304 stainless steel matrix composites reinforced with (Nb0.75, Ti0.25)C. Wear **398–399**, 220–226 (2018)
9. Velasco, F., Lima, W.M., Antón, N., Abenójar, J., Torralba, J.M.: Effect of intermetallic particles on wear behaviour of stainless steel matrix composites. Tribol. Int. **36**(7), 547–551 (2003)
10. Ni, Z., Sun, Y., Xue, F., Bai, J., Lu, Y.: Microstructure and properties of austenitic stainless steel reinforced with in situ TiC particulate. Mater. Des. **32**(3), 1462–1467 (2011)
11. Lou, D., Hellman, J., Luhulima, D., Liimatainen, J., Lindroos, V.: Interactions between tungsten carbide (WC) particulates and metal matrix in WC-reinforced composites. Mater. Sci. Eng. A **340**(1–2), 155–162 (2003)
12. Srivastava, A., Das, K.: The abrasive wear resistance of TIC and (Ti, W)C-reinforced Fe-17Mn austenitic steel matrix composites. Tribol. Int. **43**(5–6), 944–950 (2010)
13. Srivastava, A., Das, K.: Microstructural and mechanical characterization of in situ TiC and (Ti, W)C-reinforced high manganese austenitic steel matrix composites. Mater. Sci. Eng. A **516**(1–2), 1–6 (2009)
14. Knowles, A., Jiang, X., Galano, M., Audebert, F.: Microstructure and mechanical properties of 6061 Al alloy based composites with SiC nanoparticles. J. Alloys Compd. **615**(S1), S401–S405 (2014)
15. Artini, C., Muolo, M.L., Passerone, A.: Diamond-metal interfaces in cutting tools: A review. J. Mater. Sci. **47**(7), 3252–3264 (2012)
16. De Oliveira, L.J., Cabral, S.C., Filgueira, M.: Study hot pressed Fe-diamond composites graphitization. Int. J. Refract. Met. Hard Mater. **35**, 228–234 (2012)
17. Zhang, G., Xing, J., Gao, Y.: Impact wear resistance of WC/Hadfield steel composite and its interfacial characteristics. Wear **260**(7–8), 728–734 (2006)

18. Kumar, V., Venkatesh, C.: Effect of ceramic reinforcement on mechanical properties of aluminum matrix composites produced by stir casting process. Mater. Today Proc. **5**(1), 2466–2473 (2018)
19. Khmelnitsky, R., Gippius, A.: Transformation of diamond to graphite under heat treatment at low pressure. Phase Transit. **87**(2), 175–192 (2013)
20. Cunha, A., Ferreira, R., Trindade, B., Silva, F.S., Carvalho, O.: Reinforcement of a laser-textured 316L steel with CuCoBe-diamond composites through laser sintering. Mater. Manuf. Process. **35**, 1–8 (2020)
21. Cunha, A., Ferreira, R., Trindade, B., Silva, F.S., Carvalho, O.: Production of a laser textured 316L stainless steel reinforced with CuCoBe + diamond composites by hot pressing: Influence of diamond particle size on the hardness and tribological behaviour. Tribol. Int. **146**, 106056 (2020)
22. Liverani, E., Toschi, S., Ceschini, L., Fortunato, A.: Effect of selective laser melting (SLM) process parameters on microstructure and mechanical properties of 316L austenitic stainless steel. J. Mater. Process. Technol. **249**, 255–263 (2017)
23. Bartolomeu, F., et al.: 316L stainless steel mechanical and tribological behavior—A comparison between selective laser melting, hot pressing and conventional casting. Addit. Manuf. **16**, 81–89 (2017)
24. Miranda, G., Buciumeanu, M., Madeira, S., Carvalho, O., Soares, D., Silva, F.S.: Hybrid composites - metallic and ceramic reinforcements influence on mechanical and wear behavior. Compos. Part B **74**, 153–165 (2015)
25. Miranda, G., Buciumeanu, M., Carvalho, O., Soares, D., Silva, F.S.: Interface analysis and wear behavior of Ni particulate reinforced aluminum-silicon composites produced by PM. Compos. Part B **69**, 101–110 (2015)
26. Davis, C.S.: Statistical Methods for the Analysis of Repeated Measurements. Springer, New York (2002)
27. Friedman, M.: The use of ranks to avoid the assumption of normality implicit in the analysis of variance. J. Am. Stat. Assoc. **3**, 1–47 (2012)
28. Bagdonavičius, M.S., Kruopis, V., Nikulin, J.: Nonparametric Tests for Complete Data. ISTE, London; Wiley, Hoboken (2011)